Review

Tumor models for efficacy determination

Beverly A. Teicher

Genzyme Corporation, Framingham, Massachusetts

Abstract

The first *in vivo* tumor models were developed in the mid-1960s. These models were mouse leukemia models grown as ascites. The growth pattern was like that of bacteria *in vivo* and therefore it was possible to apply similar mathematics of growth and response to these tumors as had been worked out for bacteria. Since the development of the murine leukemia models, investigators have devoted a large effort to modeling solid tumors in mice. There are now a variety of models including syngeneic mouse tumors and human tumor xenografts grown as s.c. nodules, syngeneic mouse tumors and human tumor xenografts grown in orthotopic sites, models of disseminated disease, ''labeled'' tumor models that can be visualized using varied technologies, and transgenic tumor models. Each of these types of models has advantages and disadvantages to the ''drug hunter'' searching for improved treatments. [Mol Cancer Ther 2006;5(10):2435–43]

Introduction

The science of preclinical modeling of anticancer therapies began in the 1950s; however, the establishment of guidelines for experimental quality and end point rigor can be attributed in large part to the group headed by Howard Skipper at the Kettering-Meyer Laboratory affiliated with Sloan-Kettering Institute, Southern Research Institute in Birmingham, Alabama. In the mid-1960s, this group published a series of reports on the criteria of ''curability'' and on the kinetic behavior of leukemic cells in mice and the effects of anticancer chemotherapy. The principles put forward in these reports were derived directly from the behavior of bacterial cell populations exposed to antibacterial agents and were based on experimental findings in mice bearing i.p. implanted L1210 or P388 leukemia (1–11).

The initial assumptions were that (*a*) one living leukemic cell can be lethal to the host; therefore, to cure experimental leukemia, it will be necessary to kill every leukemic cell in the mouse, regardless of the number, anatomic distribution, or metabolic heterogeneity, with treatment that spares the host. (*b*) The percentage, not the absolute number, of *in vivo* leukemic cell populations of various sizes killed by a given dose of a given drug is reasonably constant. The phenomenon of a constant fractional (or percentage) drug kill of a cell population, regardless of the population size, has been observed repeatedly. (*c*) The percentage of experimental leukemic cell populations of any size killed by single-dose treatment of drug to the host is directly proportional to the dose level of the drug (i.e., the higher the dose, the higher the percentage cell kill). Thus, it is necessary to kill malignant cells faster than they are replaced by proliferation of the cells surviving the therapy if ''cure'' is to be approached (6–8).

Skipper and the group at the Kettering-Meyer Laboratory went on to develop the murine L1210 leukemia (11), as well as the murine P388 leukemia (12), into very sensitive and reasonably quantitative *in vivo* bioassay systems to study anatomic distribution and rate of leukemic cell proliferation and the effects of chemotherapy in tumor-bearing mice. These studies were based on the notion that the principle mechanism by which drug-induced increase in host life span is achieved is through leukemic cell kill, not ''inhibition of growth'' of the leukemic cell population (13). Leukemic cells that gained access to the brain and other areas of the central nervous system were not markedly affected by certain drugs; therefore, if there were leukemic cells in the central nervous system when treatment was initiated, it was necessary to employ a drug that passes the blood-brain barrier to achieve ''cure" (14, 15). A key observation was that there was a close relationship between the number of L1210 leukemic cells inoculated into BDF1 mice and the life span of these mice (13).

Antitumor activity in these early murine ascitic leukemia models was assessed on the basis of percent mean or median increase in life span, net $\log_{10}$ cell kill, and long-term survivors (16, 17). The percent mean or median increase in life span was the ratio of the survival time of treated mice (days) compared with the survival time of untreated control mice (days). Calculations of net $\log_{10}$ cell kill were made from the tumor doubling time determined from an internal tumor titration consisting of implants from serial 10-fold dilutions (Fig. 1; ref. 18). Long-term survivors were excluded from calculations of percent mean or median increase in life span and net $\log_{10}$ tumor cell kill. To assess net $\log_{10}$ tumor cell kill at the end of treatment, the survival time (days) difference between treated and control groups was adjusted to account for regrowth of tumor cell populations that may occur between individual treatments.

Received 7/6/06; revised 7/25/06; accepted 8/29/06.

Requests for reprints: Beverly A. Teicher, Genzyme Corporation, 1 Mountain Road, Framingham, MA 01701. Phone: 508-271-2843; Fax: 508-620-1203. E-mail: beverly.teicher@genzyme.com

doi:10.1158/1535-7163.MCT-06-0391

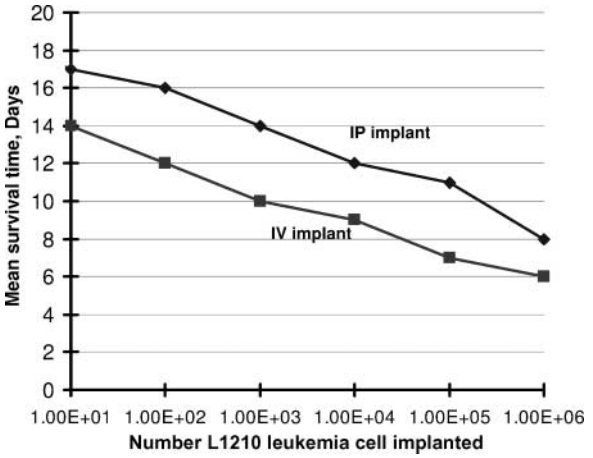

Figure 1. Mean survival time of mice inoculated with various numbers of murine L1210 leukemia cells injected i.p. or i.v. These data form the basis for the *in vivo* bioassay method for determining the number of L1201 cells surviving after treatment of L1210 tumor–bearing mice with therapy. From these survival curves, it was determined that (*i*) from i.p. inoculation, L1210 cell generation time = 0.55 day; lethal number of L1210 cells = 1.5×10^9; and (*ii*) from i.v. inoculation, L1210 cell generation time = 0.43 day (adapted from ref. 13).

Solid Tumors

As solid tumor models were developed, the appropriate end points devised were tumor growth delay or tumor control. These assays required that drugs be administered at doses producing tolerable normal tissue toxicity, so that the response of the tumor to the treatment can be observed for a relatively long period of time. Treatment with test agents was initiated either before tumor development or after a tumor nodule appeared. If treatment began the day after or the day of tumor cell implant, the experiment was a tumor growth inhibition study. If treatment began when an established tumor nodule (50–200 mm^3) was present, the experiment was a tumor growth delay study. Activity in a tumor growth delay is a stronger evidence of clinical potential than activity in a tumor growth inhibition (19, 20).

Experiments where tumor volume measurements are made over a relatively long time until the tumors reach 1.5 to 2 cm^3 allow the calculation of the tumor growth delay and percent treated versus control at multiple time points and the exponential tumor volume doubling time. Tumor growth delay is the difference in days for treated versus control tumors to reach a specified volume, usually 1 cm^3 (Fig. 2). This value is a critically important measure of antitumor effectiveness because it most closely mimics clinical end points that required observation of the mice through the time of disease progression (21, 22).

The end points applied to solid tumors require several assumptions: (*a*) the mass of a tumor is directly proportional to the number of malignant cells in the mass; (*b*) the cells killed by the test agent become nonviable promptly; and (*c*) the cells remaining viable despite treatment begin to grow again, after a relatively short lag, and proliferate at the same average rate as tumor cells in untreated control mice. Many therapies such as radiation therapy do not kill cells ''destined to die'' promptly but kill cells over several generations of proliferation, and these methods cannot be applied to such agents with accuracy. The conversion of tumor growth delay values to $\log_{10}$ cell kill is possible if the tumor maintains a log-linear growth pattern and if the volume doubling time of the tumors regrowing posttreatment approximates that of the tumors in untreated control mice (19, 22). For many tumor/treatment combinations, tumor volume provides an inaccurate measure of tumor cell kill (23). Many human tumor xenograft models do not conform to the requirement of log-linear growth and many anticancer therapies do not kill promptly with resumption of log-linear growth in the treated groups.

Response to therapies in solid tumor models can also be assessed with excision assays (23–25). Tumor excision or cell survival assays can be done if the tumor cells grow in mice and in cell culture with a good plating efficiency (1–20% or higher). The ability to measure cell survival (cell killing) from *in vivo* treatment directly is important because it gives basic information about the definitive cellular effect (Fig. 3). Tumor excision assays also allow greater accuracy and finer resolution between various therapeutic regimens than do *in situ* assays. Perhaps the greatest disadvantage of excision assays is that extended treatment regimens cannot be used due to tumor cell loss and tumor cell proliferation over the treatment time (26–31). Thus, an excision assay provides a static picture of tumor response a short time after treatment.

Syngeneic tumor models, a mouse tumor growing in mice of the strain in which the tumor originated, offer several undeniable advantages (32, 33). They are relatively low cost; reproducible; grow in immunocompetent hosts; come in a wide variety of tumor types; are generally nonimmunogenic; have a long history of use and therefore a strong baseline of drug response data; the hosts are readily available; and studies are easily conducted with statistically meaningful numbers of mice per group. The main disadvantages of syngeneic tumor models are that the tumor cells are rodent, and therefore express the mouse/rat

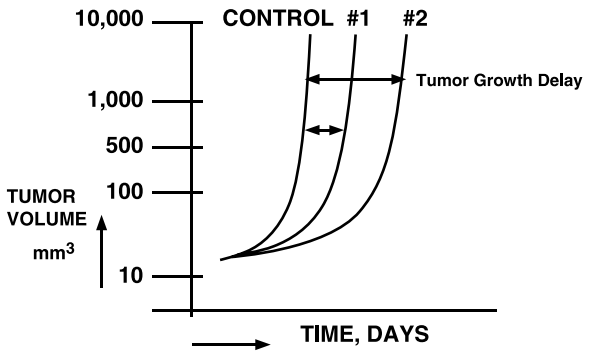

Figure 2. Schematic representation of the calculation of tumor growth delay in days is shown illustrating the log-linear relationship between tumor volume increase and time. Tumor growth delay is usually calculated when control tumors reach a volume of 500 or 1,000 mm^3.

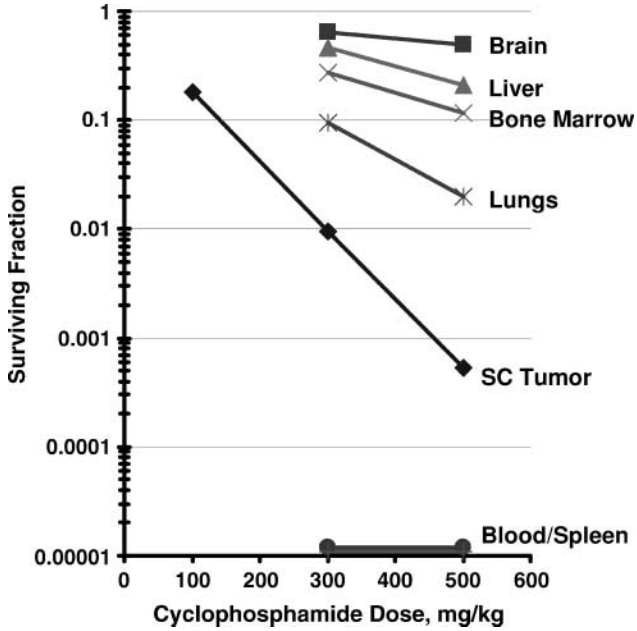

Figure 3. Survival of EMT-6 mouse mammary tumor cells located in various tissues of BALB/c mice treated with a single dose of cyclophosphamide (100, 300, or 500 mg/kg). The mice were treated with cyclophosphamide on day 7 post tumor cell implant and the tissues were excised on day 8. Plating efficiency of tumor cells from untreated control mice was set at a surviving fraction of 1.0. There is a log-linear relationship between tumor cell killing and drug dose. The large variation in response of the tumor cells to the drug depending on tissue location is evident (adapted from ref. 26).

homologues of the desired targets, and the tumors tend to grow fast. As more targeted therapies, especially antibody therapeutics, are being discovered, the homology between the human and mouse versions of the target can become a serious limiting factor for syngeneic models.

Carcinogen-induced tumors, usually in rats, have proved to be especially useful for the study of chemoprevention agents (32–34). These models, such as azoxymethane-, 3,2′-dimethyl-4-aminobiphenyl–, or *N*-methyl-*N*′-nitro-*N*-nitrosoguanidine–induced colon tumors, have enabled studies of potential chemopreventive agents for colorectal cancer (33). The *N*-nitroso-*N*-methyl urea–induced mammary carcinoma model has been instrumental in the elucidation of selective estrogen receptor modulators for the prevention of breast cancer (34). These models have also allowed the understanding of processes of mutation, oxidative stress, and inflammation that occur during carcinogenesis and the identification of new molecular targets for potential chemoprevention. These models are rarely used as cancer treatment models because the tumors are internal; there is some variability; and because the hosts are rats, a larger animal.

Human Tumor Xenografts

The development of human tumor xenograft models was a big step in moving toward more clinically relevant tumor models (35–40). The advantages of using human tumor xenografts are that the malignant cells are human; many of these models are quite reproducible; there are a wide variety of tumor lines available; many of these lines have a long history and therefore a strong baseline of drug response data; the hosts are readily available; and statistically valid numbers of mice can be used in studies. The disadvantages are that these models are more costly to run than syngeneic models; the stromal component of the tumors is rodent; the hosts are immunodeficient; most of the tumor lines were developed using early technology; and most of the time, the tumors are grown in a nonnatural site (s.c.).

Several investigators have moved away from s.c. implants and toward implanting human tumor xenografts (or syngeneic tumors) in the orthotopic site of the primary tumors from which the tumor lines were derived (41, 42). The advantages of this more refined model are that the tumor growth is in the tissue of origin of the primary tumor type; there is some variety in the tumor lines; and the hosts are readily available. The disadvantages of the orthotopic human tumor xenograft model are that the surgeries are often complex, leading to the use of low numbers of mice per study; the models are more costly; the stroma is still rodent and the tumor lines are old; the hosts are often immunodeficient; the tumor growth and response are difficult to follow and therefore survival is often the end point; and statistics are difficult. Both syngeneic and human xenograft tumors can be grown as disseminated disease either from a primary tumor implant or by intracardiac injection of tumor cells. The advantages of a disseminated disease model are that the disease pattern may more closely resemble the clinical problem because the tumor cells home to metastatic sites; there is a good variety of tumor types that can be applied in this model; and the hosts are readily available. The disadvantages are that the tumor implant requiring either a resection of a primary tumor or intracardiac injection of tumor cells is difficult and, therefore, low numbers of mice are used per study; the stroma is rodent; the growth and response of the disease are difficult to follow, often leading to a survival end point; and statistics are difficult.

"Labeled" Tumor Models

To enable orthotopic and metastatic/disseminated malignant disease to be followed, several investigators have developed ''labeled'' tumor models (43–51). These models involve the development of tumor lines that carry a foreign protein such as green fluorescence protein (GFP), red fluorescence protein (RFP), or firefly luciferase (52–55). The advantages of labeled tumor models are that the progress/response of the tumor can be followed with some form of imaging; metastasis can be visualized; internal tumor nodules can be measured; there is some variety in the tumor lines available; and the hosts are readily available. The disadvantages are that most of the tumor lines are clonal, representing a single modified cell from the original tumor line, and the clonal sublines may be a poor representation of the original disease; visualizing the

disease requires costly equipment; the stroma is rodent; and statistics are difficult. It was not long ago that Hoffman (43, 44) announced the development of human and rodent cancer cell lines that stably express GFP and produce metastatic cancer when grown in rodent. The fluorescence from the tumor cell was visualized externally by use of quantitative whole-body fluorescence imaging. The development of GFP-expressing transgenic mice followed shortly thereafter (47). The implantation of RFP-expressing B16 melanoma into GFP-expressing transgenic mice allowed the visualization of tumor-induced host processes with dual-color fluorescence imaging. Tumor cells could be definitively distinguished from host vascular cells, infiltrating cells, and stromal cells, allowing a previously unattainable look at tumor-host interactions (47). To noninvasively examine the significance of hypoxia and hypoxia-inducible factor-1 activation in incipient tumor angiogenesis, Cao et al. (52) genetically engineered HCT116 human colon carcinoma cells and 4T1 mouse mammary carcinoma cells to constitutively express RFP as a tumor marker and GFP as a reporter for hypoxia and hypoxia-inducible factor-1 activation. The mouse dorsal skin-fold window chamber was used to provide a tumor angiogenesis model that was easily visualized. The results showed that incipient tumor angiogenesis preceded the occurrence of detectable levels of hypoxia, and thus initiation of tumor angiogenesis may not depend on hypoxia or hypoxia-inducible factor-1 activation. In another application of a window chamber model, Kashiwagi et al. (53) established an *in vivo* tissue-engineered blood vessel model consisting of eGFP-HUVECs and DsRed-10T1/2 cells. This model showed that nitric oxide mediates endothelial-mural cell interaction before vessel perfusion and induces recruitment of mural cells to angiogenic vessels, vessel branching and longitudinal extension, and subsequent stabilization of vessels.

Clonal or highly selected sublines of more than 50 human tumor cells lines have been developed that express GFP, more than 25 have been developed that express RFP, and about 20 luciferase-transfected clonal sublines have been developed. In addition, clonal or highly selected sublines derived from several mouse and rat tumor lines and the hamster CHOK-1 line expressing GFP or RFP have been developed (Hoffman website). The molecular characterization of many of the GFP- and RFP-expressing sublines has been minimal. The nomenclature of the lines indicating the fluorescence protein and the tumor line from which the clone was derived may lead to the assumption that these new lines have the molecular and biological characteristics of the tumor line from which they were derived. However, these sublines should be regarded as ''new'' models and evaluated for the goodness with which they represent the human disease and must be examined individually for molecular characteristics. Using a mouse model carrying primary, genetically modified myc-driven lymphomas (murine stem cell virus–infected lymphoma cells expressing GFP, GFP/p53 null, or GFP/bcl2), Schmitt et al. (45, 46) showed that disruption of apoptosis downstream of p53 by bcl2 or a dominant-negative caspase-9 confers a selective advantage and completely alleviates pressure to inactivate p53 during lymphomagenesis. Apoptosis was the only p53 function selected against during lymphoma development. Defective cell cycle checkpoints and aneuploidy seemed to be by-products of p53 loss. To further elucidate the role of hypoxia-inducible factor in adaptation to hypoxia, Safran et al. (49) developed a genetically engineered mouse that ubiquitously expresses a bioluminescent reporter consisting of firefly luciferase fused to a region of hypoxia-inducible factor that is sufficient for oxygen-dependent degradation. This engineered mouse can be useful for monitoring hypoxic tissues and evaluating therapeutic agents that stabilize hypoxia-inducible factor. To define the role of matrix metalloproteinase-9 in tumor growth and dissemination, Acuff et al. (50) implanted luciferase-expressing human lung cancer–derived A549 cells into mice that were controls or matrix metalloproteinase-9 null. Temporal effects of stromal matrix metalloproteinase-9 expression were followed using bioluminescence imaging. As early as 19 hours after intratrachea injection, there were fewer tumor cells in the lungs of matrix metalloproteinase-9 null mice compared with control mice; however, there was no difference in subsequent tumor growth rate in the mice. Thus, matrix metalloproteinase-9 from the bone marrow seems to contribute to the early survival and establishment of lung tumors but not to the subsequent growth in the lungs. Ramesh et al. (51) developed a clonal cell line, SW780-Luc, by stably transducing the human bladder transitional cell carcinoma with a lentiviral vector coding for the luciferase gene product under control of the cytomegalovirus early gene promoter/enhancer. This tumor line was implanted orthotopically on the luminal surface of the bladder by intravesically instilling the cells in nude mice. The model was used to determine the efficacy of intravesical instillation of a conditionally replicating granulocyte macrophage colony-stimulating factor–armed oncolytic adenovirus for the treatment of bladder cancer using weekly bioluminescence imaging.

Transgenic Tumor Models

Transgenic tumor models have been available for a number of years and are growing in sophistication (56–70). These models involve tumors that arise in genetically engineered hosts. The advantages of transgenic models are that the tumor arises ''naturally'' in the host and can frequently be followed over a long time course. The disadvantages include that breeding and maintaining a colony large enough to generate sufficient numbers of mice at the same age/gender can be very costly; tumors arise at variable stages animal-to-animal and nodule-to-nodule; the stroma is rodent; the tumors are difficult to follow; the end point is frequently survival; and statistics are difficult (64–79). Most current transgenic models may be more useful for studying the biology of hyperproliferative/malignant cells than for drug discovery.

Two transgenic models, transgenic adenocarcinoma of the mouse prostate (TRAMP) and RIP/Tag2, have been

applied to therapeutic studies, albeit of limited scope. Now, several transplantable tumor lines have been developed from TRAMP tumors, making a more readily accessible mouse prostate cancer model. The RIP-Tag2 mouse is a single transgenic that is a model of islet cell carcinogenesis (64). The RIP-Tag2 model has a well-documented and relatively synchronous angiogenic switching and multistage tumorigenesis pattern that allows for testing experimental therapies in three modes: (*a*) prevention of progression of progenitor lesions to angiogenesis; (*b*) interventional treatment during the rapid phase of tumor growth; and (*c*) regression of established tumor burden (65, 66). Recently, Casanovas et al. (67) explored the therapeutic potential of antibodies to vascular endothelial growth factor (VEGF) receptor (VEGFR)-1 and VEGFR2 in controlling angiogenesis in the RIP-Tag2 model. Late-stage tumors were relatively resistant to VEGFR2 blockade because the tumor resumed growth after an initial period of growth delay. There seemed to be induction of fibroblast growth factor and other proangiogenic factors in these mice that bypassed the VEGF pathway.

In the TRAMP model, the minimal regulatory elements of the rat probasin promoter enforce prostate-specific expression of the SV40 T and t oncoproteins (68). In these mice, prostatic intraepithelial neoplasia lesions appear by 8 to 12 weeks of age, moderately differentiated carcinomas by 18 weeks of age, and poorly differentiated tumors appear by 18 to 24 weeks of age (69). Lymph node metastasis can occur as early as 12 weeks of age. The tumors begin as androgen-dependent disease at 12 weeks of age but most are androgen independent by 24 weeks of age (70, 71). The TRAMP model has been used to study tumor angiogenesis (72–74), chemoprevention (75, 76), and immunotherapy and gene therapy (77–79). Huss et al. (72) found that treatment of TRAMP mice between 10 and 16 weeks of age with the antiangiogenic kinase inhibitor SU5416 did not influence angiogenesis or tumor progression. However, treatment of TRAMP mice between 16 and 22 weeks of age with SU5416 decreased tumor-associated vessel density and increased apoptotic index and pronounced regions of cell death. In a chemoprevention study with all-*trans* retinoic acid, TRAMP mice were treated for 6 or 8 weeks at low, medium, and high dose. Although the mice developed lower grade, more differentiated tumors, there was no change in the incidence of tumors or frequency of metastasis at any dose (75).

With the development of conditional alleles that precisely mimic the mutations found in human cancers and that can be spatially and tissue-specifically controlled using ''smart'' systems, such as the tetracycline system and Cre-Lox technology, more refined engineered mouse models of the neoplastic disease process are being developed (80, 81). Although these mouse models may allow insights into the fundamental processes underlying normal and malignant cell physiology, the main purpose for developing genetically engineered mice is to model the human disease (80). To test the hypothesis of immunosurveillance, Willimsky and Blankenstein (81) generated a mouse model of sporadic cancer based on rare spontaneous activation of a dormant oncogene, SV40 T antigen. These mice spontaneously developed tumor in a variety of anatomic sites and the tumors grew progressively despite the presence of a tumor specific immune response by the host. The mice had undiminished specific B-cell responses to the tumor; however, the host T cells seemed to be anergic. Serum levels of transforming growth factor-β, which suppresses T-cell function and induces local inflammation, were increased in the tumor-bearing mice (81). Transforming growth factor-β seemed to originate from both tumor and host cells as a component of the malignant process.

Dose, Schedule, and Combination Regimens

Dose and schedule are critical determinants of drug activity (37–41). In a recent study, Graham et al. (40) evaluated the depsipeptide FK228, a histone deacetylase inhibitor, in 39 pediatric xenografts in tumor growth delay and evaluated pharmacokinetic and pharmacodynamic variables with tumor sensitivity. The results showed that FK228 inhibits its target *in vivo*; however, this effect did not correlate with sensitivity to the compound. For comparisons of time to treatment failure, survival distributions of each treatment group were compared with the survival distribution for the controls using the exact log-rank test. The relatively low objective response rate [3 of 39 (8%) tumor lines showing greater than or equal to partial response and 4 (10%) stable disease] at doses that give clinically achievable drug exposures suggests that FK228 may have limited single-agent activity in pediatric solid tumors. Keyes et al. (82, 83) measured the plasma levels of VEGF, basic fibroblast growth factor, and transforming growth factor-β in mice bearing 12 human tumor xenografts over time. Keyes et al. (83) went on to determine the effects of LY317615 (enzastaurin) on the circulating VEGF levels in mice bearing SW2 small-cell lung cancer xenografts. VEGF levels were markedly decreased in mice receiving enzastaurin; however, this change in VEGF did not correlate with tumor response. In addition to the search for better models, there remains an effort to improve methods used for determination of the additivity/synergy of drug combinations, an understanding of which is vital to developing improved cancer therapeutic regimens (84–88).

In the study of multimodality therapy or combined chemotherapy, it is of interest to determine whether the combined effects of two agents are additive or whether their combination is substantially different than the sum of their parts. Combination index methods, isobologram analysis, and uniform measures response surface analysis each provide a rigorous basis for defining regions of additivity, supra-additivity, and sub-additivity, and protection. It has been recognized that the schedule and sequence of drugs in combination can affect therapeutic outcome. Over the last 30 years, the definition of additivity and therapeutic synergism has evolved with increasing stringency. In early therapeutic modeling, therapeutic synergism between two drugs was defined to mean that ''the effect of the two drugs in combination was

significantly greater than that which could be obtained when either drug was used alone under identical conditions of treatment'' (89–92). Using this definition, the combination of cyclophosphamide and melphalan administered simultaneously by i.p. injection every 2 weeks was reported to be therapeutically synergistic in the Ridgeway osteosarcoma growth delay assay (89).

Conceptual foundations for the use of isobologram analysis of two agent combinations were based on the construction of an envelope of additivity derived from multiple isoeffect plots (isobologram; refs. 84–88). Overall, combinations that produce the desired effect and are within the boundaries of Mode I and Mode II are considered additive, those displaced to the left are supra-additive, whereas those displaced to the right are sub-additive. Combinations that produce effect outside the rectangle defined by the intersections of A_e and B_e are protective. Application of isobologram analysis requires dose (or concentration) response data for each agent alone from which the envelope (range) of additive results for the combination is calculated.

As an example, the combination of gemcitabine and navelbine was studied in the syngeneic Lewis lung carcinoma model. Gemcitabine was an active anticancer agent in mice bearing the Lewis lung carcinoma. Gemcitabine was well tolerated by the mice over the dosage range from 40 mg/kg × 3 to 80 mg/kg × 3 (Fig. 4; ref. 93). Navelbine was administered in three different well-tolerated regimens with total doses of 10, 15, and 22.5 mg/kg. Both gemcitabine and navelbine produced increasing tumor growth delay with increasing dose of the drug. To assess the efficacy of the drug combination, the intermediate dosage regimen of navelbine was combined with each dosage level of gemcitabine. These combination regimens were tolerated and the tumor growth delay increased with increasing dose of gemcitabine. The isobologram method was used to determine whether the combinations of gemcitabine and navelbine achieved additive antitumor activity. At gemcitabine doses of 40 and 60 mg/kg, the combination regimens achieved additivity, with the experimental tumor growth delay falling within the calculated envelope of additivity. At the highest dose of gemcitabine, the combination regimen produced less than additive tumor growth delay (93).

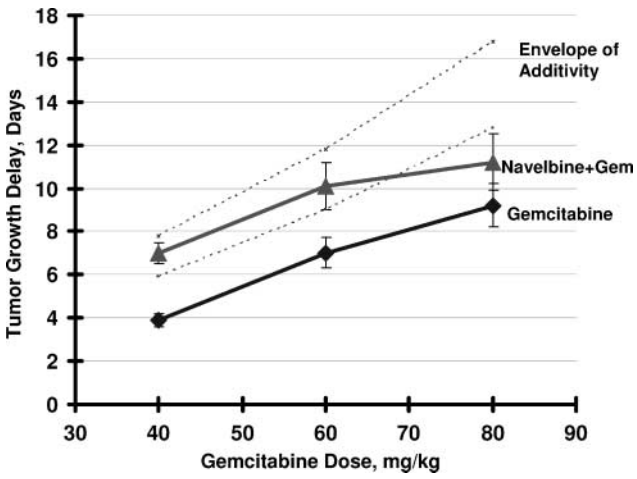

Figure 4. Growth delay of the mouse Lewis lung carcinoma produced by a range of doses of gemcitabine (i.p., days 7, 10, and 13) alone or with navelbine (15 mg/kg total dose; 10 mg/kg on day 7 and 5 mg/kg on day 14). The shaded area is the envelope of additivity calculated from dose-response curves for gemcitabine and navelbine administered as single agents using the isobologram method. *Bars,* SE (adapted from ref. 88).

The untreated control mice in this study had a mean number of 35 lung metastases on day 20. Gemcitabine was highly effective against disease metastatic to the lungs such that the mean number of lung metastases on day 20 was decreased to 1.0 to 1.5 or 3% to 4% of the number found in the untreated controls. Each of the navelbine regimens decreased the number of lung metastases on day 20 to 10 or 11 or about 30% of the number found in the untreated control mice. The combination regimens were highly effective against Lewis lung carcinoma metastatic to the lungs, with a mean number of <1 to 0 metastases found on day 20. These results support the notion that gemcitabine and navelbine may be an effective anticancer drug combination against non–small-cell lung cancer (93).

Response surface modeling provides an effective statistical approach to modeling complex patterns of synergy, additivity, and antagonism in the same data set (39, 88). Tan et al. (39) developed a class of repeated-measures models to analyze the dose-response relationship in xenograft experiments while accounting for incomplete (missing at random and informative censoring) and variable constraints. The method is based on the expectation/conditional maximization algorithm to estimate the dose-response relationship. Dose ranges of temozolomide and irinotecan and combinations of temozolomide and irinotecan were tested in the Rh18 rhabdomyosarcoma. The results showed that irinotecan was highly active whereas temozolomide had little activity in the Rh18 xenograft. The data analysis showed some evidence for synergism but it fell short of statistical significance (39).

Conclusions

The tumor response end points described in this chapter are well established and reflective of clinical outcomes in the human disease. Whereas the value of the particular tumor lines and the value of the mouse as a host remain the subject of discussion, response end points, survival end points, and tumor cell killing end points are well coordinated with clinical investigations. The s.c. implanted tumor nodule remains the mainstay of tumor models because it is easy to follow and because it has yet to be shown that orthotopic tumor models (unlabeled or labeled) would discover drugs missed by s.c. tumors. Although all of the types of tumor models discussed are being applied to drug discovery, the study of drug combinations, and to the discovery of biomarkers, transgenic tumor models primarily remain as tools to study tumor biology. Most malignant diseases are still without useful biomarkers of response to

therapies. Both imaging modalities and plasma/serum markers are being explored in the preclinical setting with hopes of developing clinically useful assays; however, examples of biomarkers/surrogate markers of tumor response remain quite rare. It is important to apply quantitative methods to the assessment of tumor growth and response to therapy and to the determination of the additivity/synergy of combination regimens.

References

1. Skipper HE. Historic milestones in cancer biology: a few that are important in cancer treatment (revisited). Semin Oncol 1979;6: 506 – 14.

2. Skipper HE. Thoughts on cancer chemotherapy and combination modality therapy. JAMA 1974;230:1033 – 5.

3. Skipper HE. Successes and failures at the preclinical level; where now? Seventh National Cancer Conference Proceedings. Philadelphia: J.B. Lippincott Company; 1973. p. 109 – 21.

4. Skipper HE. Kinetics of mammary tumor cell growth and implications for therapy. Cancer 1971;28:1479 – 99.

5. Skipper HE. Cancer chemotherapy is many things: G. H. A. Clowes memorial lecture. Cancer Res 1971;31:1173 – 80.

6. Wilcox WS, Schabel FM, Skipper HE. Experimental evaluation of potential anticancer agents. XV. On the relative rates of growth and host kill of ''single'' leukemia cells that survive *in vivo* cytoxan therapy. Cancer Res 1966;26:1009 – 14.

7. Moore GE, Sandberg AA, Ulrich K. Suspension cell culture and *in vivo* and *in vitro* chromosome constitution of mouse leukemia 1210. J Natl Cancer Inst 1966;36:405 – 21.

8. Pittilo RF, Schabel FM, Wilcox WS, Skipper HE. Experimental evaluation of potential anticancer agents. XVI. Basic study of effects of certain anticancer agents on kinetic behavior of model bacterial cell populations. Cancer Chemother Rep 1965;47:1 – 26.

9. Wilcox WS, Griswold DP, Laster WR, Schabel FM, Skipper HE. Experimental evaluation of potential anticancer agents. XVII. Kinetics of growth and regression after treatment of certain solid tumors. Cancer Chemother Rep 1965;47:27 – 39.

10. Skipper HE, Schabel FM, Wilcox WS, Laster WR, Trader MW, Thompson SA. Experimental evaluation of potential anticancer agents. XVIII. Effects of therapy on viability and rate of proliferation of leukemia cells in various anatomic sites. Cancer Chemother Rep 1965;47: 41 – 64.

11. Law LW, Dunn TB, Boyle PJ, Miller JH. Observations on the effects of a folic-acid antagonist on transplantable lymphoid leukemias in mice. J Natl Cancer Inst 1949;10:179 – 95.

12. Evans VJ, LaRock JF, Yosida TH, Potter M. A new tissue culture isolation and explanation of the P388 lymphocytic neoplasm in a chemically characterized medium. Exp Cell Res 1963;32:212 – 7.

13. Skipper HE, Schabel FM, Wilocox WS. Experimental evaluation of potential anticancer agents. XIII. On the criteria and kinetics associated with ''curability'' of experimental leukemia. Cancer Chemother Rep 1964; 35:1 – 111.

14. Rall DP. Experimental studies of the blood-brain barrier. Cancer Res 1965;25:1572 – 7.

15. Thomas LB. Pathology of leukemia in the brain and meninges: postmortem studies of patients with acute leukemia and of mice inoculated with L1210 leukemia. Cancer Res 1965;25:1555 – 71.

16. Bibby MC. Making the most of rodent tumor systems in cancer. Br J Cancer 1999;79:1633 – 40.

17. Waud WR. Murine L1210 and P388 leukemias. In: Teicher B, editor. Anticancer drug development guide: preclinical screening, clinical trials and approval. Totowa (NJ): Humana Press, Inc.; 1998. p. 59 – 74.

18. Schabel FM, Jr., Griswold DP, Jr., Laster WR, Jr., Corbett TH, Lloyd HH. Quantitative evaluation of anticancer agent activity in experimental animals. Pharmacol Ther 1977;1:411 – 35.

19. Corbett T, Valeriote F, LoRusso P, et al. *In vivo* methods for screening and preclinical testing. In: Teicher B, editor. Anticancer drug development guide: preclinical screening, clinical trials and approval. Totowa (NJ): Humana Press, Inc.; 1998. p. 75 – 99.

20. Plowman J, Dykes DJ, Hollingshead M, Simpson-Herren L, Alley MC. Human tumor xenograft models in NCI drug development. In: Teicher B, editor. Anticancer drug development guide: preclinical screening, clinical trials and approval. Totowa (NJ): Humana Press, Inc.; 1998. p. 101 – 25.

21. Teicher BA. Preclinical models for high-dose therapy. In: Teicher B, editor. Anticancer drug development guide: preclinical screening, clinical trials and approval. Totowa (NJ): Humana Press, Inc.; 1998. p. 145 – 82.

22. Corbett TH, Polin L, Roberts BJ, et al. Transplantable syngeneic rodent tumors: solid tumors in mice. In: Teicher BA, editor. Tumor models in cancer research. Totowa (NJ): Humana Press, Inc.; 2002. p. 41 – 72.

23. Teicher BA. *In vivo* tumor response end points. In: Teicher BA, editor. Tumor models in cancer research. Totowa (NJ): Humana Press, Inc.; 2002. p. 593 – 616.

24. Teicher BA, Northey D, Yuan J, Frei E, III. High-dose therapy/stem cell support: comparison of mice and humans. Int J Cancer 1996;65: 695 – 9.

25. Rockwell SC. Tumor-cell survival. In: Teicher BA, editor. Tumor models in cancer research. Totowa (NJ): Humana Press, Inc.; 2002. p. 617 – 32.

26. Teicher BA. Preclinical models for high dose therapy. In: Armitage JO, Antman KH, editors. High-dose cancer therapy: pharmacology, hematopoietins, stem cells. Baltimore: Williams and Wilkins; 1992. p. 14 – 42.

27. Teicher BA, Herman TS, Holden SA, et al. Tumor resistance to alkylating agents conferred by mechanisms operative only *in vivo*. Science 1990;247:1457 – 61.

28. Teicher BA, Holden SA, Eder JP, Brann TW, Jones SM, Frei E, III. Preclinical studies relating to the use of thiotepa in the high-dose setting alone and in combination. Semin Oncol 1990;17:18 – 32.

29. Teicher BA, Holden SA, Jones SM, Eder JP, Herman TS. Influence of scheduling on two-drug combinations of alkylating agents *in vivo*. Cancer Chemother Pharmacol 1989;25:161 – 6.

30. Teicher BA, Waxman DJ, Holden SA, et al. Evidence for enzymatic activation and oxygen involvement in cytotoxicity and antitumor activity of N,N′,N″-triethylenethiophosphoramide. Cancer Res 1989;49: 4996 – 5001.

31. Teicher BA, Frei E, III. Laboratory models to evaluate new agents for the systemic treatment of lung cancer. In: Skarin AT, editor. Multimodality treatment of lung cancer. New York: Marcel Dekker, Inc.; 2000. p. 301 – 36.

32. Sporn MB, Liby KT. Cancer chemoprevention: scientific promise, clinical uncertainty. Nat Clin Pract Oncol 2005;2:518 – 25.

33. Corpet DE, Tache S. Most effective colon cancer chemopreventive agents in rats: a systematic review of aberrant crypt foci and tumor data, ranked by potency. Nutr Cancer 2002;43:1 – 21.

34. Sporn MB, Dowsett SA, Mershon J, Bryant HU. Role of raloxifene in breast cancer prevention in post menopausal women: clinical evidence and potential mechanisms of action. Clin Ther 2004;26:830 – 40.

35. Kelland LR. ''Of mice and men'': values and liabilities of the athymic nude mouse model in anticancer drug development. Eur J Cancer 2004; 40:827 – 36.

36. Sausville EA, Newell DR. Preclinical models in cancer drug discovery and development. Eur J Cancer 2004;40:783 – 4.

37. Peterson JK, Houghton PJ. Integrating pharmacology and *in vivo* cancer models in preclinical and clinical drug development. Eur J Cancer 2004;40:837 – 44.

38. Peterson JK, Tucker C, Favours E, et al. *In vivo* evaluation of ixabepilone (BMS247550), a novel epothilone B derivative, against pediatric cancer models. Clin Cancer Res 2005;11:6950 – 8.

39. Tan M, Fang H-B, Tian G-L, Houghton PJ. Repeated-measures models with constrained parameters for incomplete data in tumor xenograft experiments. Stat Med 2005;24:109 – 19.

40. Graham C, Tucker C, Creech J, et al. Evaluation of the antitumor efficacy, pharmacokinetics and pharmacodynamics of the histone deacetylase inhibitor depsipeptide in childhood cancer models *in vivo*. Clin Cancer Res 2006;12:223 – 34.

41. Kerbel RS. Human tumor xenografts as predictive preclinical models for anticancer drug activity in humans: better than commonly perceived—but they can be improved. Cancer Biol Ther 2003;2:S134 – 9.

42. Bibby MC. Orthotopic models of cancer for preclinical drug evaluation: advantages and disadvantages. Eur J Cancer 2004;40:852 – 7.

43. Hoffman RM. Visualization of GFP-expressing tumors and metastasis *in vivo*. Biotechniques 2001;30:1016 – 26.

44. Hoffman RM. Green fluorescent protein imaging of tumor growth, metastasis and angiogenesis in mouse models. Lancet Oncol 2002;3: 546 – 56.

45. Schmitt CA, Fridman JS, Yang M, Baranov E, Hoffman RM, Lowe SW. Dissecting p53 tumor suppressor function *in vivo*. Cancer Cell 2002; 1:289 – 98.

46. Schmitt CA, Fridman JS, Yang M, et al. A senescence program controlled by p53 and $p16^{INK4a}$ contributes to the outcome of cancer therapy. Cell 2002;109:335 – 46.

47. Yang M, Li L, Jiang P, Moossa AR, Penman S, Hoffman RM. Dual-color fluorescence imaging distinguishes tumor cells from induced host angiogenic vessels and stromal cells. Proc Natl Acad Sci U S A 2003;100: 14259 – 62.

48. John CM, Leffler H, Kahl-Knutsson B, Svensson I, Jarvis GA. Truncated galectin-3 inhibits tumor growth and metastasis in orthotopic nude mouse model of human breast cancer. Clin Cancer Res 2003;9: 2374 – 83.

49. Safran M, Kim WY, O'Connell F, et al. Mouse model for noninvasive imaging of HIF prolyl hydroxylase activity: assessment of an oral agent that stimulates erythropoietin production. Proc Natl Acad Sci U S A 2006; 103:105 – 10.

50. Acuff HB, Carter KJ, Fingleton B, Gorden DL, Matrisian LM. Matrix metalloproteinase-9 from bone marrow-derived cells contributes to survival but not growth of tumor cells in the lung microenvironment. Cancer Res 2006;66:259 – 66.

51. Ramesh N, Ge Y, Ennist DL, et al. CG0070, a conditionally replicating granulocyte macrophage colony-stimulating factor-armed oncolytic adenovirus for the treatment of bladder cancer. Clin Cancer Res 2006;12: 305 – 13.

52. Cao Y, Li C-Y, Moeller BJ, et al. Observation of incipient tumor angiogenesis that is independent of hypoxia and hypoxia inducible factor-1 activation. Cancer Res 2005;65:5498 – 505.

53. Kashiwagi S, Izumi Y, Gohongi T, et al. NO mediates mural cell recruitment and vessel morphogenesis in murine melanomas and tissue-engineered blood vessels. J Clin Invest 2005;115:1816 – 27.

54. Kisucka J, Butterfield CE, Duda DG, et al. Platelets and platelet adhesion support angiogenesis while preventing excessive hemorrhage. Proc Natl Acad Sci U S A 2006;103:855 – 60.

55. Duda DG, Cohen KS, di Tomaso E, et al. Differential CD146 expression on circulating versus tissue endothelial cells in rectal cancer patients: implications for circulating endothelial and progenitor cells as biomarkers for antiangiogenic therapy. J Clin Oncol 2006;24:1449 – 53.

56. Hansen K, Khanna C. Spontaneous and genetically engineered animals models: use in preclinical cancer drug development. Eur J Cancer 2004;40:858 – 80.

57. Dinulescu DM, Ince TA, Quade BJ, Shafer SA, Crowley D, Jacks T. Role of K-ras and Pten in the development of mouse models of endometriosis and endometrioid ovarian cancer. Nat Med 2005;11: 63 – 70.

58. Jackson EL, Olive KP, Tuveson DA, et al. The differential effects of mutant p53 alleles on advanced murine lung cancer. Cancer Res 2005;65: 10280 – 8.

59. Grimm J, Kirsch DG, Windsor SD, et al. Use of gene expression profiling to direct *in vivo* molecular imaging of lung cancer. Proc Natl Acad Sci U S A 2005;102:14404 – 9.

60. Wijnhoven SWP, Zwart E, Speksnijder EN, et al. Mice expressing a mammary gland-specific R270H mutation in the p53 tumor suppressor gene mimic human breast cancer development. Cancer Res 2005;65: 8166 – 73.

61. Bender Kim CF, Jackson EL, Woolfenden AE, et al. Identification of bronchioalveolar stem cells in normal lung and lung cancer. Cell 2005;121: 823 – 35.

62. Hill R, Song Y, Cardiff RD, Van Dyke T. Selective evolution of stromal mesenchyme with p53 loss in response to epithelial tumorigenesis. Cell 2005;123:1001 – 11.

63. Gutmann DH, Maher EA, Van Dyke T. Mouse models of human cancers consortium workshop on nervous system tumors. Cancer Res 2006;66:10 – 3.

64. Hanahan D. Heritable formation of pancreatic B-cell tumors in transgenic mice expressing recombinant insulin/simian virus 40 oncogenes. Nature 1985;315:115 – 22.

65. Bergers G, Javaherian K, Lo KM, Folkman J, Hanahan D. Effects of angiogenesis inhibitors on multistage carcinogenesis in mice. Science 1999;284:808 – 12.

66. Bergers G, Song S, Meyer-Morse N, Bergsland E, Hanahan D. Benefits of targeting both pericytes and endothelial cells in the tumor vasculature with kinase inhibitors. J Clin Invest 2003;111:1287 – 95.

67. Casanovas O, Hicklin DJ, Bergers G, Hanahan D. Drug resistance by evasion of antiangiogenic targeting of VEGF signaling in late-stage pancreatic islet tumors. Cancer Cell 2005;8:299 – 309.

68. Greenberg NM, DeMayo F, Finegold MJ, et al. Prostate cancer in a transgenic mouse. Proc Natl Acad Sci U S A 1995;92:3439 – 43.

69. Kaplan-Leftko PJ, Chen TM, Ittmann MM, et al. Pathobiology of autochthonous prostate cancer in a preclinical transgenic mouse model. Prostate 2003;55:219 – 37.

70. Gingrich JR, Barrios RJ, Kattan MW, Nahm HS, Finegold MJ, Greenberg NM. Androgen-independent prostate cancer progression in the TRAMP model. Cancer Res 1997;57:4687 – 91.

71. Morgenbesser SD, McLaren RP, Richards B, et al. Identification of genes potentially involved in the acquisition of androgen-independent and metastatic tumor growth in an autochthonous genetically engineered mouse prostate cancer model. Prostate. In press 2006.

72. Huss WJ, Barrios RJ, Greenberg NM. SU5416 selectively impairs angiogenesis to induce prostate cancer-specific apoptosis. Mol Cancer Ther 2003;2:611 – 6.

73. Ozawa MG, Yao VJ, Chanthery YH, et al. Angiogenesis with pericyte abnormalities in a transgenic model of prostate carcinoma. Cancer 2005; 104:2104 – 15.

74. Ozerdem U. Targeting of pericytes diminishes neovascularization and lymphangiogenesis in prostate cancer. Prostate 2006;66:294 – 304.

75. Huss WJ, Lai L, Barrios RJ, Hirschi KK, Greenberg NM. Retinoic acid slows progression and promotes apoptosis of spontaneous prostate cancer. Prostate 2004;61:142 – 52.

76. McCabe MT, Low JA, Daignault S, Imperiale MJ, Wojno KJ, Day ML. Inhibition of DNA methyltransferase activity prevents tumorigenesis in a mouse model of prostate cancer. Cancer Res 2006;66: 385 – 92.

77. Fukuhara H, Martuza RL, Rabkin SD, Ito Y, Todo T. Oncolytic herpes simplex virus vector G47Δ in combination with androgen ablation for the treatment of human prostate adenocarcinoma. Clin Cancer Res 2005;11: 7886 – 90.

78. Varghese S, Rabkin SD, Liu R, Nielsen PG, Ipe T, Martuza RL. Enhanced therapeutic efficacy of IL-12, but not GM-CSF, expressing oncolytic herpes simplex virus for transgenic mouse derived prostate cancers. Cancer Gene Ther 2006;13:253 – 65.

79. Zhang Q, Yang X, Pins M, et al. Adoptive transfer of tumor-reactive transforming growth factor-β-insensitive $CD8^+$ T cells: eradication of autologous mouse prostate cancer. Cancer Res 2005;65:1761 – 9.

80. Maddison K, Clarke AR. New approaches for modeling cancer mechanisms in the mouse. J Pathol 2005;205:181 – 93.

81. Willimsky G, Blankenstein T. Sporadic immunogenic tumors avoid destruction by inducing T-cell tolerance. Nature 2005;437:141 – 6.

82. Keyes KA, Mann L, Cox K, Treadway P, Iversen P, Teicher BA. Circulating angiogenic growth factor levels in mice bearing human tumors using Luminex multiplex technology. Cancer Chemother Pharmacol 2003; 51:321 – 7.

83. Keyes KA, Mann L, Sherman M, et al. LY317615 decreases plasma VEGF levels in human tumor xenograft-bearing mice. Cancer Chemother Pharmacol 2004;53:133 – 40.

84. Steel GG, Peckham MJ. Exploitable mechanisms in combined radiotherapy-chemotherapy: the concept of additivity. Int J Radiat Oncol Biol Phys 1979;5:85 – 91.

85. Berenbaum MC. Synergy, additivism and antagonism in immunosuppression. Clin Exp Immunol 1977;28:1 – 18.

86. Dewey WC, Stone LE, Miller HH, Giblak RE. Radiosensitization with 5-bromodeoxyuridine of Chinese hamster cells x-irradiated during different phases of the cell cycle. Radiat Res 1977;47:672 – 88.

87. Deen DF, Williams MW. Isobologram analysis of X-ray-BCNU interactions *in vitro*. Radiat Res 1979;79:483 – 91.

88. White DB, Slocum HK, Brun Y, Wrzosek C, Greco WR. A new nonlinear mixture response surface paradigm for the study of synergism: a three drug example. Curr Drug Metab 2003;4:399 – 409.

89. Schabel FM, Trader MW, Laster WR, Wheeler GP, Witt MH. Patterns of resistance and therapeutic synergism among alkylating agents. Antibiot Chemother (Basel) 1978;23:200 – 15.

90. Schabel FM, Griswold DP, Corbett TH, Laster WR, Mayo JG, Lloyd HH. Testing therapeutic hypotheses in mice treated with anticancer drugs that have demonstrated or potential clinical utility for treatment of advanced solid tumors of man. Methods Cancer Res 1979;17:3 – 51.

91. Schabel FM, Jr., Griswold DP, Jr., Corbett TH, Laster WR, Jr. Increasing therapeutic response rates to anticancer drugs by applying the basic principles of pharmacology. Pharmacol Ther 1983;20:283 – 305.

92. Griswold DP, Corbett TH, Schabel FM, Jr. Clonogenicity and growth of experimental tumors in relation to developing resistance and therapeutic failure. Cancer Treat Rep 1981;65:51 – 4.

93. Herbst RS, Lynch C, Vasconcelles M, et al. Gemcitabine and vinorelbine in patients with advanced lung cancer: preclinical studies and report of a phase I trial. Cancer Chemother Pharmacol 2001;48: 151 – 9.

Molecular Cancer Therapeutics

Tumor models for efficacy determination

Beverly A. Teicher

Mol Cancer Ther 2006;5:2435-2443.